Integrated Multi-Omics Analyses Reveal the Molecular Basis of Tryptophol Over-Accumulation in Saccharomyces Cerevisiae

Xiaowei Gong
China Tobacco Yunnan Industrial Corporation
Huajun Luo
Kunming University of Science and Technology
Liu Hong
China Tobacco Yunnan Industrial Corporation
Jun Wu
China Tobacco Yunnan Industrial Corporation
Chunxia Song
Kunming University of Science and Technology
Wei Zhao
China Tobacco Yunnan Industrial Corporation
Wenyu Wu
Kunming University of Science and Technology
Yi Han
China Tobacco Yunnan Industrial Corporation
Ya Dao
Kunming University of Science and Technology
Xia Zhang
China Tobacco Yunnan Industrial Corporation
Donglai Zhu
China Tobacco Yunnan Industrial Corporation
Yiyong Luo (yyongl-168@163.com)
Kunming University of Science and Technology https://orcid.org/0000-0002-0273-9218

Research

Keywords: Saccharomyces cerevisiae, Tryptophol, Metabolomics, Genomics, Transcriptomics, Nitrogen catabolite repression

Posted Date: November 19th, 2020

DOI: https://doi.org/10.21203/rs.3.rs-108779/v1

Abstract

Background

Tryptophol (TOL) is a metabolic derivative of tryptophan (Trp) and shows pleiotropic effects in humans, plants and microbes. The mechanisms of TOL biosynthesis were first explored several decades ago. Nonetheless, a systematic interpretation of TOL over-accumulation is still lacking.

Results

Based on TOL yield, a suitable transformation medium (TM1) was used to culture *Saccharomyces cerevisiae* strain KMLY1-2. The dynamics of TOL production, cell growth, and gene transcription revealed that TOL production was dependent on cell density and the expression of key genes. Additionally, the effects of Trp and phenylalanine (Phe) on TOL production were tested, and the results showed that Trp can significantly facilitate TOL accumulation, but output plateaued (231.02–266.31 mg/L) at Trp concentrations ≥0.6 g/L. In contrast, Phe reduced the stimulatory effect of Trp, which strongly depended on the Phe concentration. To elucidate the molecular basis and regulatory mechanism of TOL overproduction, an integrated analysis of metabolomics, genomics, and transcriptomics was performed. The results revealed that 1) both the Ehrlich pathway and tryptamine-dependent pathway were involved in *S. cerevisiae* TOL biosynthesis; 2) Trp increased TOL production by enhancing the Ehrlich pathway, in which the steps of transamination (including aminotransferase genes *aro9*, *aat1*, *bat2* and *his5*) and decarboxylation (including decarboxylase genes *aro10* and *pdc5*) played important roles. Of course, this process was assisted by amino acid permease genes *agp1* and *tat2*, dihydrolipoyl dehydrogenase gene *lpd1*, and transcriptional activator gene *aro80*, etc.; 3) Phe restricted TOL biosynthesis by repressing the transcript levels of genes such as *aat1*, *his5*, *aro10*, *pdc5* and *aro80*, thus interfering with the transamination and decarboxylation reactions; and 4) under sufficient Trp conditions, the de novo Trp biosynthetic pathway and central carbon metabolism (glycolysis, pentose phosphate pathway, and citrate cycle) of *S. cerevisiae* were weakened, while the content of some amino acids increased, which may be related to the promotion of yeast cell growth by Trp.

Conclusions

In this study, TOL production of *S. cerevisiae* was significantly improved, and our integrated multi-omics analyses have provided insights into the understanding of TOL over-accumulation, which will be useful for future production of TOL using metabolic engineering strategies.

Background

Tryptophol (TOL, i.e., indole-3-ethanol), with a molecular formula of $C_{10}H_{11}NO$ and molecular weight of 161.2, is an aromatic alcohol widely found in wine, beer and other beverages [1]. Similar to most indole compounds, TOL has multiple biological activities. For instance, TOL is able to induce apoptosis in human leukaemia U937 cells without affecting normal lymphocytes [2], and can attenuate pathogen-

induced inflammation-related responses of the cytokines TNFα and IFNγ [3]. In addition to the potential bioactivity for humans, TOL is a growth promoting factor for roots and leaves of plants [4]; it can inhibit viral replication of white spot syndrome of the shrimp *Marsupenaeus japonicus* [5], and it possesses antimicrobial activity against the food contaminants *Campylobacter jejuni* [6] and *Salmonella enterica* [7]. Therefore, research on TOL biosynthesis and regulation has attracted widespread attention.

TOL, similar to two other aromatic alcohols (2-phenylethanol and tyrosol), is biosynthesized through the well-known Ehrlich pathway through three enzymatic steps: transamination, decarboxylation and reduction. More specifically, tryptophan (Trp) is first transaminated by aromatic aminotransferases I and II, which are encoded by the genes *aro8* and *aro9*, respectively [8]. The formed Indole-3-pyruvate (IPA) is then catalysed by an aromatic decarboxylase (ARO10) and three pyruvate decarboxylases (PDC1, PDC5 and PDC6), and alcohol dehydrogenases (ADHs) encoded by *adh1−5* and *sfa1* are proposed to be involved in the final step of the Ehrlich pathway [8]. TOL can also be biosynthesized de novo from glucose [9]. In this process, phosphoenolpyruvate (PEP) from glycolysis and erythrose 4-phosphate (E4P) from pentose phosphate pathway enter shikimate pathway to form chorismate, which is then converted to Trp via five enzymatic reactions and further catabolized to TOL through the Ehrlich pathway.

Many microorganisms including plant-beneficial bacteria, filamentous fungi and yeast can produce TOL [8, 10-12]. Among these microbes, yeast has the strongest TOL production capacity, with a maximum yield of approximately 580 mg/L, which was produced by *Zygosaccharomyces priorianus* [13]. *Saccharomyces cerevisiae* can also produce large amounts of TOL, with an output of up to 478 mg/L when Trp was the only nitrogen source [8]. The fact that Trp has notable effects on TOL production has also been reported in some other yeast species. For example, TOL in *Debaryomyces hansenii* was synthesized only when Trp was present in the medium [14], and in *Candida albicans*, the production of TOL increased by 2.5 times after the addition of Trp [15]. Moreover, the influence of other nitrogen sources, not only Trp, on TOL production has long been recognized. González et al. found that nitrogen limitation strongly promoted the production of aromatic alcohols [10], whereas high ammonium conditions dramatically reduced them [16].

To clarify the molecular mechanisms behind the nitrogen effects, expression levels of genes in the Ehrlich pathway were investigated. It has been reported that *aro9* and *aro10* gene transcription was induced by the presence of Trp, phenylalanine (Phe), and tyrosine in the growth medium, and this induction required the transcriptional activator ARO80 and resulted in TOL, 2-phenylethanol, and tyrosol accumulation, respectively [16, 17]. Importantly, the biosynthetic TOL activates ARO80 and, consequently, the expression of *aro9* and *aro10*, resulting in a positive feedback loop [16]. Similarly, nitrogen-poor conditions promote the expression of *aro9*, *aro10* and *pdc6*, whereas high ammonia or abundant nitrogen represses them [16]. Additionally, some genes involved in cofactor metabolism, transcriptional regulation, and amino acid transportation were reported to influence the biosynthesis of aromatic alcohols. Dickinson et al. found that the titre of TOL obviously decreased in a dihydrolipoyl dehydrogenase gene (*lpd1*) mutant, meaning that LPD1 was required for Trp catabolism to TOL [8]. Similarly, THI3, a sensor of intracellular thiamine pyrophosphate (TPP), was required along with pyruvate decarboxylases for the alternative activity [18]. In

addition to ARO80, CAT8 and MIG1 are two well-documented transcription factors. It has been reported that *cat8* overexpression or *mig1* deletion increased the transcription of *aro9* and *aro10*, followed by an enhanced formation of 2-phenylethanol [19]. In addition, amino acid permease genes *agp1*, *agp2*, *tat1* and *tat2* are transcriptionally induced by extracellular aromatic amino acids, and GATA factors such as GLN3 and GAT1 regulate the transcription of *aro9* and *aro10* for nitrogen source and aromatic amino acid utilization [20, 21]. To fully understand the biosynthetic process of TOL, it should be considered that genes other than those of the Ehrlich pathway and de novo biosynthetic pathway are used in an auxiliary pathway.

Recently, multi-omics analyses, including genomics, transcriptomics and metabolomics, have been used to gain an in-depth understanding of the Trp-dependent biosynthesis of indole-3-acetic acid (IAA), an auxin sharing a common direct precursor, indole-3-acetaldehyde (IAD), with TOL, in some plant-associated microbes [11]. In this work, to systematically clarify the molecular basis of TOL over-accumulation, a *S. cerevisiae* strain KMLY1-2 (hereafter referred to as KMLY1-2) with high TOL production ability was screened out, and its yield dynamics over varying Trp concentrations were monitored. Moreover, the differential effect of Trp and Phe on TOL biosynthesis was investigated, and the molecular mechanism behind TOL overproduction was elucidated by multi-omics analyses. Our current findings may help to further improve the yield of TOL through metabolic engineering strategies and lay a foundation for industrial production of TOL with high efficiency.

Results And Discussion

TM1 is a suitable medium for TOL production

To select a culture medium for TOL production, KMLY1-2 was cultured in transformation medium (TM) containing different carbon and nitrogen sources (Table S1). No TOL was produced in TM1 and TM2, and the highest yield (only 1.66 mg/L) was detected in TM4 (Fig. S1a). After an addition of 1 g/L Trp, the yield of TOL in TM1 and TM2, two media without nitrogen, was significantly increased, with TM1 resulting in the highest yield of 236.68 mg/L. In addition, TOL production decreased with the increasing nitrogen content in TM3-1Trp–TM5-1Trp, with the yield of TOL in TM5-1Trp being approximately 4.93% of that in TM1-1Trp (Fig. S1b). The data indicated that, except for Trp, high nitrogen was not conducive to TOL production, which is highly consistent with a previous report by Chen and Fink [16]. Therefore, TM1, due to the absence of nitrogen and high-yield TOL, was chosen for subsequent experiments.

TOL production is dependent on cell density and the expression of key genes

Yeast growth and TOL production were measured over time. As shown in Fig. 1a, 0–24 and 24–42 h were identified as the exponential phase and stationary phase, respectively, according to the time–OD_{600} curve. Additionally, the TOL content sharply increased from 0–24 h and stayed constant from 24–42 h. Among them, the TOL concentration at 24 h was 211.46 mg/L. The highly consistent data of TOL production and cell growth indicated that TOL production is closely related to cell density. To clarify whether this process

requires TOL biosynthetic genes, four key genes (*aro8*, *aro9*, *aro10* and *aro80*) were selected and their expression levels were analysed. The expression of *aro8*, *aro10* and *aro80* gradually increased from 0 h to 18 h, while that of *aro9* peaked at 12 h and slightly decreased at 18 h. In addition, these genes showed stable expression levels after 24 h (Fig. 1b). The profile of key gene expression is consistent, to a certain extent, with the pattern of TOL production and growth, indicating that the phenomenon of TOL yield dependence on cell density requires the expression of aromatic aminotransferases (ARO8 and ARO9), a decarboxylase (ARO10) and a transcription factor (ARO80), which is partly congruent with reports by Chen and Fink [16]. Therefore, 24 h is a critical time point and is considered to be the fermentation time of KMLY1-2 in the subsequent experiments.

TOL production is dependent on Trp and Phe concentrations

To explore the effects of Trp and Phe on TOL biosynthesis, TOL production was monitored after KMLY1-2 was incubated in TM1 with different concentrations of Trp and Phe. As shown in Fig. 2a, TOL yield increased proportionally as the Trp concentration increased but was more or less flat (231.02–266.31 mg/L) when ≥0.6 g/L Trp was supplied to the medium. Meanwhile, increasing amounts of residual Trp accumulated accordingly. These data indicated that the ability of KMLY1-2 to convert Trp into TOL was saturated from 0.6 g/L Trp. However, Phe did not affect TOL production when it was the sole nitrogen source in the medium (data not shown), which was ascribed to Phe being a direct precursor for 2-phenylethanol biosynthesis [9]. In addition, TOL content was significantly reduced when KMLY1-2 was cultured in TM1 containing Trp and Phe as nitrogen sources, and the reduction was strongly dependent on the Phe concentration (Fig. 2b). This may be attributed to nitrogen catabolite repression (NCR) in which high ammonia restricts TOL production by repressing the transcript level of genes in the Ehrlich pathway [10, 16]. However, the mechanism of Phe affecting the conversion of Trp to TOL is still unclear. In contrast with the results of extracellular TOL, a significantly different effect of 0.6 and 1.5 Trp on intracellular TOL production was observed (Fig. 2c). This discrepancy was mainly due to differences in biomass, as the intracellular TOL yield was calculated by weight normalization.

Metabolomic profiles

The chemical profile of the KMLY1-2 endometabolome was generated by liquid chromatography/mass spectrometry, and a total of 4473 metabolites with definite names were identified. Principal component analysis (PCA) and orthogonal partial least squares discriminant analysis (OPLS-DA) showed that the sample replicates were tightly clustered and the samples from different media were clearly separated (Fig. S2), suggesting that the metabolomic data were highly reproducible. Of these metabolites, 1011, 1201, 281 and 694 differential metabolites (DMs), including 30, 30, 14 and 11 compounds of Trp and its derivatives, were identified in TM *vs*. TM-06T, TM *vs*. TM-15T, TM-06T *vs*. TM-15T, and TM-06T *vs*. TM-TP, respectively (Table S2). The Kyoto Encyclopedia of Genes and Genomes (KEGG) enrichment analysis of DMs showed that biosynthesis of antibiotics (ko01130) was the only shared enriched pathway in TM *vs*. TM-06T, TM *vs*. TM-15T and TM-06T *vs*. TM-TP (Table S2), suggesting that the addition of Trp and Phe to the medium may affect the biosynthesis of some antibiotics [22]. In addition, the abundance of DMs in

the Ehrlich pathway and its bypass of Trp metabolism was analysed. As shown in Fig. 3, intracellular L-Trp abundance, as expected, increased with the increase in exogenous Trp concentration, which was not different between TM-06T and TM-TP, indicating that Phe had no effect on Trp transportation. A similar abundance trend for intracellular Trp was observed in IPA, IAD, tryptamine and IAA, suggesting that both the Ehrlich pathway and the tryptamine-dependent pathway (Trp→tryptamine→IAD) are involved in TOL biosynthesis of *S. cerevisiae*, as reported for the fungus *Neurospora crassa* [23], although the functional genes in the tryptamine pathway have not been identified in *S. cerevisiae*. In addition, the ranges of the increases in IPA and IAD abundance from TM to TM-06T were respectively smaller than those of L-Trp and IPA, while the decline ratios of IPA and IAD abundance from TM-06T to TM-TP were larger than that of L-Trp (Fig. 3a). The former indicates that transamination and decarboxylation are two rate-limiting steps in TOL biosynthesis, while the latter shows that these steps are susceptible to Phe, which may result in the NCR phenomenon of TOL biosynthesis due to Phe or phenylpyruvate (PPA) competing with Trp or IPA for the active centre of transaminase and decarboxylase, respectively. For the analysis of TOL abundance, the peak value was identified in TM-06T, which is highly consistent with the intracellular high-performance liquid chromatography (HPLC) data in Fig. 2c. The relatively low abundance in TM-15T may be ascribed to the reversible conversion of TOL to IAD by alcohol dehydrogenase, followed by convertion to IAA by aldehyde dehydrogenase. Different from the effect of Phe on the abovementioned metabolites, Phe promoted indolelactate accumulation (Fig. 3b), and the reason should be further studied.

General features of the KMLY1-2 genome

PacBio sequencing generated an assembled nuclear genome containing 31 contigs with 11.79 Mbp (~113 × coverage) and 38.1% GC content, similar to previously reported *S. cerevisiae* strains [24]. A total of 5539 protein-coding sequences (CDSs) with an average length of 1476 bp were predicted, representing 69.31% of the genome. In addition, 3 rRNA and 315 tRNA were identified in the genome. Among all the predicted proteins, 5537, 5527, 2733 and 3795 CDSs were allocated to the non-redundant protein (Nr), swiss-prot, eukaryotic orthologous groups of proteins (KOG), and KEGG databases, respectively, based on sequence homologies, yielding 2376 shared annotated CDSs in total. According to the KEGG annotation, the pathways for glycolysis, citrate cycle, pentose phosphate cycle, amino acids biosynthesis, and purine and pyrimidine metabolism were complete. Furthermore, the candidate genes involved in TOL biosynthesis in KMLY1-2 and S288C (a model *S. cerevisiae* strain) were subjected to a comparative analysis. As shown in Table 1, a complete Ehrlich pathway, containing seven aminotransferases, four decarboxylases, and seven dehydrogenases, which showed sufficient homology (98.66–100%, except for ADH3), were identified. Genomic blast analysis showed that the *adh3* gene in KMLY1-2 was highly homologous to four consecutive genes in S288C (*adh3*, YMR084W, YMR085W and *seg1*), indicating that it is a tetrafunctional polypeptide. Additionally, nine proteins (ARO1–ARO4 and TRP1–TRP5) with 97.93–100% identity were responsible for Trp biosynthesis from E4P and PEP via chorismate, meaning that both KMLY1-2 and S288C have the complete de novo biosynthetic pathway of TOL. Similarly, genes in the auxiliary pathway showed high homology (83.8–99.89%) between KMLY1-2 and S288C, suggesting that these genes are also conserved in yeast. Nevertheless, the TOL yield of KMLY1-2 was approximately

1.57 times than that of S288C when they were cultivated in TM1 supplemented with 1.5 g/L Trp, which may be attributed to the different regulatory mechanisms during TOL biosynthesis.

Transcriptome sequencing and analysis of differentially expressed genes (DEGs)

With the aim of dissecting the molecular mechanism of yeast TOL biosynthesis and regulation, transcriptome sequencing and analysis of TM, TM-06T, TM-15T and TM-TP were performed. Approximately 36623732–89449834 clean reads (99.82–99.93% of raw reads) were generated in 12 RNA-seq libraries, and 89.74–96.06% of the total reads mapped to the KMLY1-2 reference genome, among which 45.69–81.24% were CDS mapped reads (Table S3). A correlation analysis of three replicates showed high biological reproducibility (average Pearson correlation coefficient of 0.98). The transcript levels determined by the average FPKM (fragment per kilobase of transcript per million mapped reads) values showed that 5495, 5492, 5383 and 5288 genes were expressed in TM, TM-06T, TM-15T and TM-TP, respectively. According to the criteria described in the methods, there were 2183, 2068, 43, 2297, 1018 and 527 DEGs in the comparisons TM *vs.* TM-06T, TM *vs.* TM-15T, TM-06T *vs.* TM-15T, TM *vs.* TM-TP, TM-06T *vs.* TM-TP, and TM-15T *vs.* TM-TP, respectively (Fig. S3a). Since there were no shared DEGs in these comparisons, we divided them into group I (TM *vs.* TM-06T and TM *vs.* TM-15T) and II (TM-06T *vs.* TM-TP and TM-15T *vs.* TM-TP), and 1447 shared DEGs in group I, 253 in group II, and 201 in group I and II were identified (Fig. S3b), which may be closely associated with the fact that Trp facilitated TOL accumulation and Phe reduced TOL production. Using the short time series expression miner (STEM) algorithms, these shared DEGs can be clustered in 17 profiles (Fig. S3c–e). The transcript levels of DEGs in profile 1 were in a pattern of “increase-keep-decrease” from TM to TM-06T and TM-15T to TM-TP, which perfectly matched the data of extracellular TOL yield in Fig. 2a and b. Further analyses showed that one aminotransferase (HIS5), two decarboxylases (ARO10 and PDC5), a chorismate synthase (ARO2), and the transcriptional activator ARO80, which have been proven to participate in aromatic alcohols biosynthesis [8, 9, 20], were contained in profile 1 (Table S4). Additionally, eight and two genes speculated to participate in the Ehrlich, de novo, and auxiliary biosynthetic pathways of TOL were identified in profile 9 and profile 14, respectively (Table S4). Considering the fact that genes with similar expression patterns might be functionally correlated [25], it is reasonable to assume that genes in profiles 1 and 9, profiles 1 and 14 may be highly related to TOL production and the NCR phenomenon, respectively. In fact, eight and five TPP metabolism genes, coding for essential cofactors for PDC1, PDC5 and ARO10 [26], were respectively identified in profiles 1 and 9. Additionally, an aldehyde dehydrogenase, which functions in the conversion of IAD to IAA [11] and showed a relatively low expression level in TM-TP, gives an alternative reason why Phe decreased IAA abundance (Fig. 3b) and has been identified in profile 14 (Table S4). These data further confirmed that genes in profiles 1 and 9 were closely related to aromatic alcohol biosynthesis and regulation, and genes in profile 14 were responsible for NCR in *S. cerevisiae*.

Expression profile analyses of the DEGs involved in TOL biosynthesis

As shown in Fig. 4, when Trp was used as the sole nitrogen source, four of five aminotransferases, two of four PPA or pyruvate decarboxylases, and two of three alcohol dehydrogenases in the Ehrlich pathway showed an upward trend, indicating that these enzymes played important roles in the biosynthesis of TOL; while the transcript levels of these transaminase and decarboxylase genes decreased when Trp and Phe were present in the same medium, which was similar to the fact that abundant nitrogen downregulated *aro9* and *aro10* gene expression as reported by Chen and Fink [16]. An alternative, but non-exclusive, explanation for NCR can be given based on the expression patterns of *aro9* and *aro10*. Phe, Trp, and TOL (a degradation metabolite of Trp) can upregulate the expression of *aro9* and *aro10* [16]; hence, the promoting effect of Trp on *aro9* and *aro10* transcripts was stronger than that of Phe. When Phe and Trp are present simultaneously, they will compete for metabolic enzymes in the Ehrlich pathway of *S. cerevisiae*, and Phe is a preferentially used amino acid [27], causing the pathway of Trp to IAD to be blocked, meaning that the expression of *aro9* and *aro10* is only regulated by Phe. Therefore, the gene expression level in TM-TP is lower than that in TM-06T and TM-15T. For the de novo biosynthesis pathway, the transcription levels of six DEGs first increased and then decreased sharply, with TM-06T as the turning point, which indicated that these genes tended to make cells synthesize more Trp at low concentrations of extracellular Trp, while the expression of these genes was suppressed by feedback in the presence of high concentrations of amino acids. In addition, the expression of gene 3726 (*aro1*) was more susceptible to exogenous Trp, and its expression level was inhibited once the exogenous environment contained Trp. For the auxiliary pathway, Trp promoted the expression abundance of three amino acid transporters, but there was no difference between TM-06T and TM-TP, which perfectly matched the metabolomics data in Fig. 3a, indicating again that Phe and Trp do not compete with the cell transport system. In addition, the expression levels of *lpd1* (1892) and *aro80* (4004) showed a trend consistent with the production of extracellular TOL, suggesting that they did play an important role in the biosynthesis of TOL in *S. cerevisiae*. However, the transcript levels of *mig1* (5390), *cat8* (3322) and *gln3* (4745) decreased with the increase in nitrogen concentration, indicating that they were negatively correlated with the biosynthesis of TOL. This was partly the same as and partly contrary to the results reported by Wang et al. [19], and the reasons need to be further determined.

Integrated metabolomics and transcriptomics analyses

To fully understand the molecular mechanism of TOL overproduction in *S. cerevisiae*, the metabolism of amino acids, especially Trp, and the central carbon metabolism (glycolysis, pentose phosphate pathway, and citrate cycle) containing DMs and/or DEGs were summarized and described in Fig. 5. As expected, the abundance of metabolites and expression levels of most genes in the Ehrlich pathway in TM-06T and TM-15T were significantly increased compared with TM. For instance, the contents of TOL, IAD and IPA in TM-06T and TM-15T were 3.97–253.69 times more than those in TM. Consistently, the transcript levels of *aro9*, *pdc5*, *aro10*, *adh2* and *adh5* increased 2.19–376.46 times (Table S5). The results indicated that the addition of Trp increased TOL biosynthesis by enhancing the Ehrlich pathway, and genes with large changes, such as *aro9* (353.15 to 376.46 folds), *pdc5* (30.2 to 49.16 folds), and *aro10* (205.74 to 222.96 folds), may have made important contributions. However, some metabolites and genes in the Ehrlich pathway showed a decreased trend after Phe was added to TM-06T (i.e., sample TM-TP), in which the

content of TOL and the expression levels of *his5*, *aat1*, *aro10*, and *pdc5* in TM-TP were 34.26% and 19.63–43.81% of those in TM-06T, respectively (Table S5). The results suggested that Phe addition weakened the Ehrlich pathway of TOL biosynthesis, which may be attributed to the inhibition of Trp to TOL by Phe competition because Phe is a preferred nitrogen source in *S. cerevisiae*.

In addition, the abundance of most metabolites in other branches of Trp metabolism in TM-06T or TM-15T was, as expected, significantly higher than that in TM. For example, a 2.74–34.76-fold increase was identified for indole-3-acetonitrile, 5-hydroxy-tryptophan and N-formylkynurenine (Table S5). Most strikingly, except for gene *bna2* (0177), which showed 5.83 and 6.11 times higher transcript levels in TM-06T and TM-15T, respectively, compared with those in TM, the transcript levels of other related genes mostly decreased to different degrees (Table S5). The somewhat inconsistent results between metabolomic and transcriptomic data has often been reported, which might be related to the complex post-transcriptional mechanisms after gene transcription [28, 29].

For other amino acids, compared with TM, 10 amino acids, including serine, arginine and others displayed 2.05–74.19-folds increases in TM-06T or TM-15T. Moreover, alanine, valine and tyrosine increased their abundance by 3.24-, 2.56- and 5.06-fold, respectively, in the comparison of TM-06T *vs.* TM-TP (Table S5). These increases may be due to the addition of Trp and Phe providing cells with more energy and precursors, which promotes the biosynthesis of other amino acids and consequently results in cell growth. The fact that KMLY1-2 biomass increased significantly after Trp and Phe were added to TM1 (Fig. S4) further supports this speculation. In this context, the rapid growth of yeast cells will undoubtedly consume more carbon sources. Indeed, compared with TM, the abundance of many intermediate metabolites in the glycolysis, the pentose phosphate pathway and the citrate cycle was significantly reduced in TM-06T or TM-15T, and the expression levels of corresponding genes also showed a decreasing trend (Fig. 5). The lack of significant changes in glucose content may be attributed to hexokinase (1820), an important regulatory enzyme in central carbon metabolism [30], whose transcription level decreased significantly in TM-06T and TM-15T (Table S5), thus limiting the efficient utilization of glucose.

Conclusions

In summary, we designed a suitable transformation medium for TOL yield evaluation, and found that TOL production was dependent on cell density and the expression of key genes of *S. cerevisiae*. To improve TOL output, we added Trp and Phe to TM1 and found that TOL production increased proportionally as the exogenous Trp concentration increased, while Phe attenuated the stimulating effect of Trp. In addition, the effect of Trp on TOL was saturated from ≥0.6 g/L supplemental Trp, and 231.02–266.31 mg/L TOL was obtained in this situation. We also performed a multi-omics analysis to understand how yeast cells over-accumulated TOL. Our data revealed that the Ehrlich pathway was the main pathway for yeast TOL biosynthesis, in which the steps of transamination and decarboxylation played key roles in the biosynthesis of TOL and in the phenomenon of nitrogen catabolite repression conferred by Phe. In addition, TOL over-accumulation was inseparable from the help of the auxiliary pathway and many other

genes. In short, our findings provide a rich genetic resource for the subsequent studies on the biosynthesis of Trp metabolites in *S. cerevisiae*.

Materials And Methods

Chemicals, yeast strain and media

L-Trp, L-Phe, TOL and 2-chlorophenylalanine were purchased from Sigma-Aldrich (St. Louis, MO), and chromatographic grade methanol and acetonitrile were obtained from Sangon Biotech Co., Ltd. (Shanghai, China). *S. cerevisiae* strain KMLY1-2 was isolated by our laboratory from homemade sourdough and cultivated in de Man, Rogosa and Sharpe (MRS) medium (HKM, Guangdong, China). TM1−5 (Table S1) and TM1−5 supplemented with 1 g/L Trp were used for TOL production.

HPLCdetection of TOL production

The seed culture of KMLY1-2 (10^6 CFU/mL) was inoculated (1%, v/v) in 50 mL MRS medium and incubated at 35 °C for 12 h in an agitating incubator (150 rpm). Cells were harvested by centrifugation at 5000 rpm for 10 min and re-suspended in 5 mL sterile ddH_2O after washing twice with sterile ddH_2O. The cell suspension was inoculated (1%, v/v) in 100 mL TM1−5 and cultivated with a shaking speed of 150 rpm at 35 °C for 24 h. Cell-free supernatant (CFS) from 1 mL culture was prepared by centrifugation (12000 rpm for 10 min; 4 °C) and sterile filtration using a 0.45 μm filter (Millipore, Billerica, MA), and used for TOL content determination using an HPLC system (Agilent Technologies, Santa Clara, CA). Briefly, aliquots of 10 μL were loaded into an Acclaim Explosives E2 column (4.6 × 250 mm, 5 μm, 120 Å; Thermo Scientific, Waltham, MA). Isogradient elution was performed using methanol/H_2O solution (70:30, v/v) for 20 min at a temperature of 25 °C and a flow rate of 0.5 mL/min. TOL were monitored at 210 nm, and their concentrations were determined by integrating the calibration curves obtained from the standards. Each sample was performed at least in triplicate.

Time course analysis of cell growth, TOL production, and expression of key genes

KMLY1-2 was pre-cultured in MRS medium and re-suspended in sterile ddH_2O as described above. The cell suspension was inoculated (1%, v/v) in 100 mL TM1 supplemented with 0.5 g/L Trp and incubated for 42 h. OD_{600}, representing cell growth, was monitored every 6 h. Meanwhile, the CFS and cell pellets were collected and used for TOL content measurement and quantitative PCR (qPCR) assay, respectively. Total RNA extraction, cDNA synthesis, and qPCR were performed according to our previous study [31]. The primers are listed in Table S6, and differences in expression of genes *aro8*, *aro9*, *aro10* and *aro80* were calculated according to the $2^{-\Delta\Delta CT}$ method [32] using the actin gene (*act1*) as the reference.

TOL production under Trp and Phe conditions

KMLY1-2 was pre-treated as described above and incubated in TM1 supplemented with 0−2.5 g/L Trp. To evaluate the effects of both Trp and Phe on TOL production, KMLY1-2 was cultured in TM1 supplemented

with 0.6–1.5 g/L Trp and 0–2.25 g/L Phe. After incubation for 24 h, the CFS was prepared as described above and analysed by HPLC to quantify the produced TOL and the residual Trp. Accordingly, cell pellets from TM1 and TM1 supplemented with 0.6 g/L Trp, 1.5 g/L Trp, or 0.6 g/L Trp and 1.75 g/L Phe were collected to generate the samples of TM, TM-06T, TM-15T, and TM-TP, respectively. To test the intracellular TOL concentration, all cell pellets were weighed, ground with liquid nitrogen, and re-suspended with 0.95 mL sterile ddH_2O. After centrifugation and filtration treatment, the TOL level in the filtrate was reflected by the value of TOL/weight (μg/g). All assays were carried out at least in triplicate.

Intracellular metabolomics analysis

Cell pellets of TM, TM-06T, TM-15T, and TM-TP (each 50 mg) were re-suspended in 1000 μL of cold acetonitrile-methanol-water (2:2:1, v/v) containing 1 μg/mL 2-chlorophenylalanine as an internal standard. The extraction and determination of metabolites were conducted exactly as described by Xu et al. [33]. The raw data detected by UHPLC-Q-Exactive-Orbitrap-MS was converted to the mzML format and analysed by R package XCMS (version 3.2) for peak identification and matching. The peak area of each metabolite was normalized to the internal standard, and the normalized data from five replicates for each sample was subjected to multivariate statistical analysis, including PCA and OPLS-DA, using the SIMCA-P package (Umetrics, Umea, Sweden). DMs between two samples were identified according to the restrictive conditions of fold change ≥2 and a corrected *p*-value <0.05.

Genome sequencing, assembly and annotation

Genomic DNA of KMLY1-2 was extracted using a yeast genome DNA extraction kit (Tiangen, China) and sequenced on the PacBio RS II platform. Briefly, the qualified genomic DNA was fragmented with Covaris G-tubes and end-repaired to prepare single-molecule real-time (SMRT) bell DNA template libraries (insert size of >10 Kb) according to the manufacturer's specifications (PacBio, Menlo Park, CA). SMRT sequencing was performed on the PacBio RSII sequencer using P4-C2 chemistry. The long seed reads were corrected and assembled as described by Frank et al. [34]. Finally, the assembled sequences (scaffolds) were deposited in GenBank under accession number JADIFZ000000000, and applied as the draft genome sequence of KMLY1-2. CDSs were predicted using AUGUSTUS [35], and their annotations were performed using BLASTP search against the Nr, Swiss-Prot, KOG, and KEGG databases. In addition, rRNA and tRNA prediction was performed by RNAmmer [36] and tRNAscan-SE [37], respectively.

RNA extraction, library construction and sequencing

Total RNAs from the samples TM, TM-06T, TM-15T, and TM-TP were extracted using a trizol reagent kit (Invitrogen, Carlsbad, CA) according to the manufacturer's instructions, and 12 high-quality RNA samples were used to construct RNA-seq libraries using the TruSeq RNA sample preparation kit (Illumina, San Diego, CA) following the manufacturer's protocol. Then, the libraries were sequenced using Illumina HiSeq 4000 to generate 100 nt paired-end raw reads. The raw data were deposited in the short read archive database under accession number SRR12995594–SRR12995605. Clean reads were selected by a Perl

program according to the criteria described by Wu et al. [38] and mapped to the genome of KMLY1-2 using HISAT2 [39] with default settings.

Analysis of DEGs

Aligned reads were quantified using an FPKM method [40]. DEGs between two samples were identified using DESeq2 [41] following two criteria: an absolute value of $\log_2$ fold change ≥1 and a false discovery rate (FDR) <0.05. The DEGs were then subjected to clustering analysis by using the STEM algorithms [42]. Finally, the DMs and DEGs involved in TOL biosynthesis in KEGG pathways were selected for integrative analysis.

Abbreviations

TOL: tryptophol; Trp: tryptophan; IPA: Indole-3-pyruvate; ADHs: alcohol dehydrogenases; PEP: phosphoenolpyruvate; E4P: erythrose 4-phosphate; Phe: phenylalanine; TPP: thiamine pyrophosphate; IAA: indole-3-acetic acid; IAD: indole-3-acetaldehyde; TM: transformation medium; NCR: nitrogen catabolite repression; PCA: principal component analysis; OPLS-DA: orthogonal partial least squares discriminant analysis; KEGG: kyoto encyclopedia of genes and genomes; DMs: differential metabolites; PPA: phenylpyruvate; HPLC: high-performance liquid chromatography; CDSs: protein-coding sequences; Nr: non-redundant protein; KOG: eukaryotic orthologous groups of proteins; DEGs: differentially expressed genes; FPKM: fragment per kilobase of transcript per million mapped reads; STEM: short time series expression miner; FDR: false discovery rate; CFS: Cell-free supernatant; SMRT: single-molecule real-time; qPCR: quantitative PCR.

Declarations

Acknowledgements

Not applicable.

Authors' contributions

XG, DZ and YL conceived and designed the study. HL, LH, JW, WW and YD conducted the experiments. XG, CS, WZ and YH analysed the data and drafted the manuscript. XG, XZ and YL revised the manuscript. All authors read and approved the final manuscript.

Funding

This work was supported by the National Natural Science Foundation of China (32060531 and 31660451), the Young Academic and Technical Leader Raising Foundation of Yunnan Province (to Yiyong Luo), the Ten-thousand Talents Program in Yunnan province (to Yiyong Luo), and the Key Scientific Research Project of China Tobacco Yunnan Industrial Co., Ltd. (2020XY01).

Availability of data and materials

The datasets used and/or analysed during the current study are available from the corresponding author on reasonable request.

Ethics approval and consent to participate

Not applicable.

Consent for publication

Not applicable.

Competing interests

The authors declare that they have no competing interests.

References

1. Palmieri A, Petrini M. Tryptophol and derivatives: natural occurrence and applications to the synthesis of bioactive compounds. Nat Prod Rep. 2019;36(3):490–530.
2. Inagaki S, Morimura S, Gondo K, Tang Y, Akutagawa H, Kida K. Isolation of tryptophol as an apoptosis-inducing component of vinegar produced from boiled extract of black soybean in human monoblastic leukemia U937 cells. Biosci Biotechnol Biochem. 2007;71(2):371–9.
3. Schirmer M, Smeekens SP, Vlamakis H, Jaeger M, Oosting M, Franzosa EA, et al. Linking the human gut microbiome to inflammatory cytokine production capacity. Cell. 2016;167(4):1125–36.
4. do Nascimento ALV, Macedo WR, Silva GH, de Almeida Neto RG, Mendes MG, Marchiori PER. Physiological and agronomical responses of common bean subjected to tryptophol. Ann Appl Biol. 2016;168:195–202.
5. Zhu F, Jin M. The effects of a thermophile metabolite, tryptophol, upon protecting shrimp against white spot syndrome virus. Fish Shellfish Immunol. 2015;47(2):777–81.
6. Gañan M, Martínez-Rodríguez AJ, Carrascosa AV. Antimicrobial activity of phenolic compounds of wine against *Campylobacter jejuni*. Food Control. 2009;20(8):739–42.
7. Elleuch L, Shaaban M, Smaoui S, Mellouli L, Karray-Rebai I, Fourati-Ben Fguira L, et al. Bioactive secondary metabolites from a new terrestrial *Streptomyces* sp. TN262. Appl Biochem Biotechnol. 2010;162(2):579–93.
8. Dickinson JR, Salgado LE, Hewlins MJ. The catabolism of amino acids to long chain and complex alcohols in *Saccharomyces cerevisiae*. J Biol Chem. 2003;278(10):8028–34.
9. Hassing EJ, de Groot PA, Marquenie VR, Pronk JT, Daran JG. Connecting central carbon and aromatic amino acid metabolisms to improve de novo 2-phenylethanol production in *Saccharomyces cerevisiae*. Metab Eng. 2019;56:165–80.

10. Gonzalez B, Vazquez J, Morcillo-Parra MA, Mas A, Torija MJ, Beltran G. The production of aromatic alcohols in non-*Saccharomyces* wine yeast is modulated by nutrient availability. Food Microbiol. 2018;74:64–74.
11. Li M, Guo R, Yu F, Chen X, Zhao H, Li H, et al. Indole-3-acetic acid biosynthesis pathways in the plant-beneficial bacterium *Arthrobacter pascens* ZZ21. Int J Mol Sci. 2018;19(2):443.
12. Luo K, DesRoches CL, Johnston A, Harris LJ, Zhao HY, Ouellet T. Multiple metabolic pathways for metabolism of l-tryptophan in *Fusarium graminearum*. Can J Microbiol. 2017;63(11):921–7.
13. Rosazza JP, Juhl R, Davis P. Tryptophol formation by *Zygosaccharomyces priorianus*. Appl Microbiol. 1973;26(1):98–105.
14. Gori K, Knudsen PB, Nielsen KF, Arneborg N, Jespersen L. Alcohol-based quorum sensing plays a role in adhesion and sliding motility of the yeast *Debaryomyces hansenii*. FEMS Yeast Res. 2011;11(8):643–52.
15. Ghosh S, Kebaara BW, Atkin AL, Nickerson KW. Regulation of aromatic alcohol production in *Candida albicans*. Appl Environ Microbiol. 2008;74(23):7211–8.
16. Chen H, Fink GR. Feedback control of morphogenesis in fungi by aromatic alcohols. Genes Dev. 2006;20(9):1150–61.
17. Iraqui I, Vissers S, Andre B, Urrestarazu A. Transcriptional induction by aromatic amino acids in *Saccharomyces cerevisiae*. Mol Cell Biol. 1999;19(5):3360–71.
18. Vuralhan Z, Morais MA, Tai SL, Piper MD, Pronk JT. Identification and characterization of phenylpyruvate decarboxylase genes in *Saccharomyces cerevisiae*. Appl Environ Microbiol. 2003;69(8):4534–41.
19. Wang Z, Bai X, Guo X, He X. Regulation of crucial enzymes and transcription factors on 2-phenylethanol biosynthesis via Ehrlich pathway in *Saccharomyces cerevisiae*. J Ind Microbiol Biotechnol. 2017;44(1):129–39.
20. Chen X, Wang Z, Guo X, Liu S, He X. Regulation of general amino acid permeases Gap1p, GATA transcription factors Gln3p and Gat1p on 2-phenylethanol biosynthesis via Ehrlich pathway. J Biotechnol. 2017;242:83–91.
21. Regenberg B, During-Olsen L, Kielland-Brandt MC, Holmberg S. Substrate specificity and gene expression of the amino-acid permeases in *Saccharomyces cerevisiae*. Curr Genet. 1999;36(6):317–28.
22. Brakhage AA. Molecular regulation of beta-lactam biosynthesis in filamentous fungi. Microbiol Mol Biol Rev. 1998;62(3):547–85.
23. Sardar P, Kempken F. Characterization of indole-3-pyruvic acid pathway-mediated biosynthesis of auxin in *Neurospora crassa*. PLoS One. 2018;13(2):e0192293.
24. Song G, Dickins BJ, Demeter J, Engel S, Gallagher J, Choe K, et al. AGAPE (Automated Genome Analysis PipelinE) for pan-genome analysis of *Saccharomyces cerevisiae*. PLoS One. 2015;10(3):e0120671.

25. Yang J, Yin ZQ, Kang ZT, Liu CJ, Yang JK, Yao JH, et al. Transcriptomic profiling of *Alternaria longipes* invasion in tobacco reveals pathogenesis regulated by AlHK1, a group III histidine kinase. Sci Rep. 2017;7(1):16083.
26. Mojzita D, Hohmann S. Pdc2 coordinates expression of the THI regulon in the yeast *Saccharomyces cerevisiae*. Mol Genet Genomics. 2006;276(2):147–61.
27. Beltran G, Novo M, Rozes N, Mas A, Guillamon JM. Nitrogen catabolite repression in *Saccharomyces cerevisiae* during wine fermentations. FEMS Yeast Res. 2004;4(6):625–32.
28. Udomsom N, Rai A, Suzuki H, Okuyama J, Imai R, Mori T, et al. Function of AP2/ERF transcription factors involved in the regulation of specialized metabolism in *Ophiorrhiza pumila* revealed by transcriptomics and metabolomics. Front Plant Sci. 2016;7:1861.
29. Kanani H, Dutta B, Klapa MI. Individual *vs.* combinatorial effect of elevated CO_2 conditions and salinity stress on *Arabidopsis thaliana* liquid cultures: comparing the early molecular response using time-series transcriptomic and metabolomic analyses. BMC Syst Biol. 2010;4:177.
30. Wang J. Glycolysis. In: Wang J, Zhu S, Xu C, editors. Biochemistry. 3rd ed. Beijing: Higher Education Press; 2002. p. 63–91.
31. Dao Y, Zhang K, Lu X, Lu Z, Liu C, Liu M, et al. Role of glucose and 2-oxoglutarate/malate translocator (OMT1) in the production of phenyllactic acid and *p*-hydroxyphenyllactic acid, two food-borne pathogen inhibitors. J Agric Food Chem. 2019;67(20):5820–6.
32. Livak KJ, Schmittgen T. Analysis of relative gene expression data using real-time quantitative PCR and the 2(-Delta Delta C(T)) method. Methods. 2001;25(4):402–8.
33. Xu C, Liu X, Zha H, Fan S, Zhang D, Li S, et al. A pathogen-derived effector modulates host glucose metabolism by arginine GlcNAcylation of HIF-1alpha protein. PLoS Pathog. 2018;14(8):e1007259.
34. Frank J, Dingemanse C, Schmitz AM, Vossen RH, van Ommen GJ, den Dunnen JT, et al. The complete genome sequence of the murine pathobiont *Helicobacter typhlonius*. Front Microbiol. 2016;6:1549.
35. Stanke M, Morgenstern B. AUGUSTUS: a web server for gene prediction in eukaryotes that allows user-defined constraints. Nucleic Acids Res. 2005;33(suppl_2):W465–7.
36. Lagesen K, Hallin P, Rodland EA, Staerfeldt HH, Rognes T, Ussery DW. RNAmmer: consistent and rapid annotation of ribosomal RNA genes. Nucleic Acids Res. 2007;35(9):3100–8.
37. Lowe TM, Eddy SR. tRNAscan-SE: a program for improved detection of transfer RNA genes in genomic sequence. Nucleic Acids Res. 1997;25(5):955–64.
38. Wu W, Deng G, Liu C, Gong X, Ma G, Yuan Q, et al. Optimization and multiomic basis of phenyllactic acid overproduction by *Lactobacillus plantarum*. J Agric Food Chem. 2020;68(6):1741–9.
39. Kim D, Langmead B, Salzberg SL. HISAT: a fast spliced aligner with low memory requirements. Nat Methods. 2015;12(4):357–60.
40. Pertea M, Kim D, Pertea GM, Leek JT, Salzberg SL. Transcript-level expression analysis of RNA-seq experiments with HISAT, StringTie and Ballgown. Nat Protoc. 2016;11(9):1650–67.

41. Love MI, Huber W, Anders S. Moderated estimation of fold change and dispersion for RNA-seq data with DESeq2. Genome Biol. 2014;15(12):550.
42. Ernst J, Bar-Joseph Z. STEM: a tool for the analysis of short time series gene expression data. BMC Bioinformatics. 2006;7:191.

Tables

Table 1 Identity of possible genes involved in TOL biosynthesis in KMLY1-2 and S288C genome

Pathways	Name in KMLY1-2	Name in S288C	Identity (%)	Products and entry numbers in KEGG	Description
Ehrlich pathway	5539	YGL202W	99.93	ARO8/Aromatic amino acid aminotransferase I (EC 2.6.1.57; 2.6.1.28)	Conversion of Trp to IPA
	1736	YHR137W	99.29	ARO9/Aromatic amino acid aminotransferase II (EC 2.6.1.57; 2.6.1.28)	
	0955	YKL106W	99.93	AAT1/Aspartate aminotransferase, mitochondrial (EC 2.6.1.1)	
	2416	YLR027C	99.6	AAT2/Aspartate aminotransferase, cytoplasmic (EC 2.6.1.1)	
	4561	YIL116W	99.48	HIS5/Histidinol-phosphate aminotransferase (EC 2.6.1.9)	
	1808	YHR208W	99.75	BAT1/Branched chain amino acid aminotransferase (EC 2.6.1.42)	
	0244	YJR148W	99.29	BAT2/Branched chain amino acid aminotransferase (EC 2.6.1.42)	
	3966	YDR380W	99.53	ARO10/Phenylpyruvate decarboxylase (EC 4.1.1.43)	Conversion of IPA to IAD
	2431	YLR044C	99.65	PDC1/Pyruvate decarboxylase isozyme I (EC 4.1.1.1)	
	2517	YLR134W	99.41	PDC5/Pyruvate decarboxylase isozyme II (EC 4.1.1.1)	
	5285	YGR087C	98.7	PDC6/Pyruvate decarboxylase isozyme III (EC 4.1.1.1)	
	1613	YOL086C	98.76	ADH1/NADH-alcohol dehydrogenase isozyme I (EC 1.1.1.1)	Conversion of IAD to TOL
	3300	YMR303C	98.66	ADH2/NADH-alcohol dehydrogenase isozyme II (EC 1.1.1.1)	
	3511	YMR083W	17.41	ADH3/NADH-alcohol dehydrogenase isozyme III (EC 1.1.1.1)	
	2849	YGL256W	99.83	ADH4/NADH-alcohol dehydrogenase isozyme IV (EC 1.1.1.1)	
	4345	YBR145W	99.81	ADH5/NADH-alcohol dehydrogenase isoenzyme V (EC 1.1.1.1)	
	3283	YMR318C	100	ADH6/$NADP^+$-alcohol dehydrogenase (EC 1.1.1.2)	

	0332	YDL168W	99.57	SFA1/Bifunctional alcohol dehydrogenase/S-(hydroxymethyl)glutathione dehydrogenase (EC 1.1.1.1; EC 1.1.1.284)

Table 1 ***Continued***

Pathways	Name in KMLY1-2	Name in S288C	Identity (%)	Products and entry numbers in KEGG	Description
De novo bio-synthetic pathway	0519	YDR035W	97.93	ARO3/3-deoxy-7-phosphoheptulonate synthase (EC 2.5.1.54)	Conversion of E4P and PEP to chorismate
	4441	YBR249C	99.55	ARO4/3-deoxy-7-phosphoheptulonate synthase (EC 2.5.1.54)	
	3726	YDR127W	99.69	ARO1/Pentafunctional AROM polypeptide (EC 4.2.3.4; 4.2.1.10; 1.1.1.25; 2.7.1.71; 2.5.1.19)	
	5490	YGL148W	99.38	ARO2/Chorismate synthase (EC 4.2.3.5)	
	4691	YER090W	99.48	TRP2/Anthranilate synthase (EC 4.1.3.27)	Conversion of chorismate to Trp
	3942	YDR356W	99.22	TRP4/Anthranilate phosphoribosyltransferase (EC 2.4.2.18)	
	0494	YDR007W	100	TRP1/Phosphoribosylanthranilate isomerase (EC 5.3.1.24)	
	1047	YKL211C	99.59	TRP3/Indole-3-glycerol phosphate synthase (EC 4.1.1.48)	
	5383	YGL026C	99.58	TRP5/Tryptophan synthase (EC 4.2.1.20)	
Auxiliary pathway	1892	YFL018C	99.67	LPD1/Dihydrolipoyl dehydrogenase (EC 1.8.1.4)	Cofactor metabolism
	1141	YDL080C	99.02	THI3/Thiamine pyrophosphate sensor	
	4004	YDR421W	99.12	ARO80/Transcriptional activator	Transcriptional regulation
	3322	YMR280C	98.84	CAT8/Regulatory protein	
	5390	YGL035C	99.67	MIG1/Regulatory protein	
	4745	YER040W	99.22	GLN3/Nitrogen regulatory protein	
	1894	YFL021W	83.8	GAT1/Transcriptional regulatory protein	
	1956	YCL025C	99.32	AGP1/General amino acid permease I	Amino acid transportation

4334	YBR132C	99.44	AGP2/General amino acid permease II
4274	YBR069C	99.89	TAT1/Aromatic amino-acid permease I
1188	YOL020W	99.33	TAT2/Aromatic amino-acid permease II

Figures

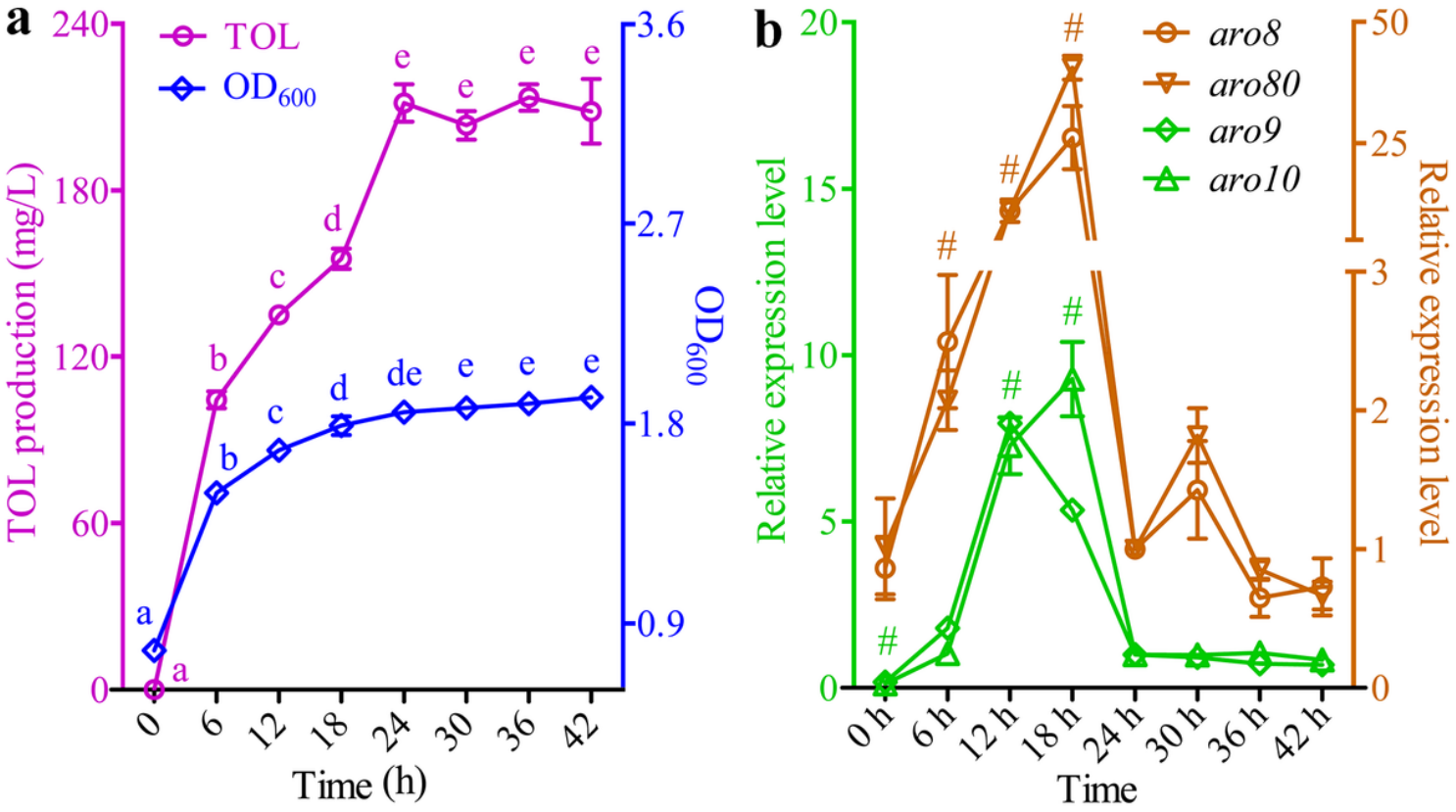

Figure 1

Kinetics curves of TOL production and cell growth (a), and relative expression levels of TOL key biosynthetic genes (b). Different lowercase letters (a to e) indicate significant differences ($p < 0.05$). The expression level at 24 h was set as 1, and # denotes the fold change relative to 24 h ≥2.

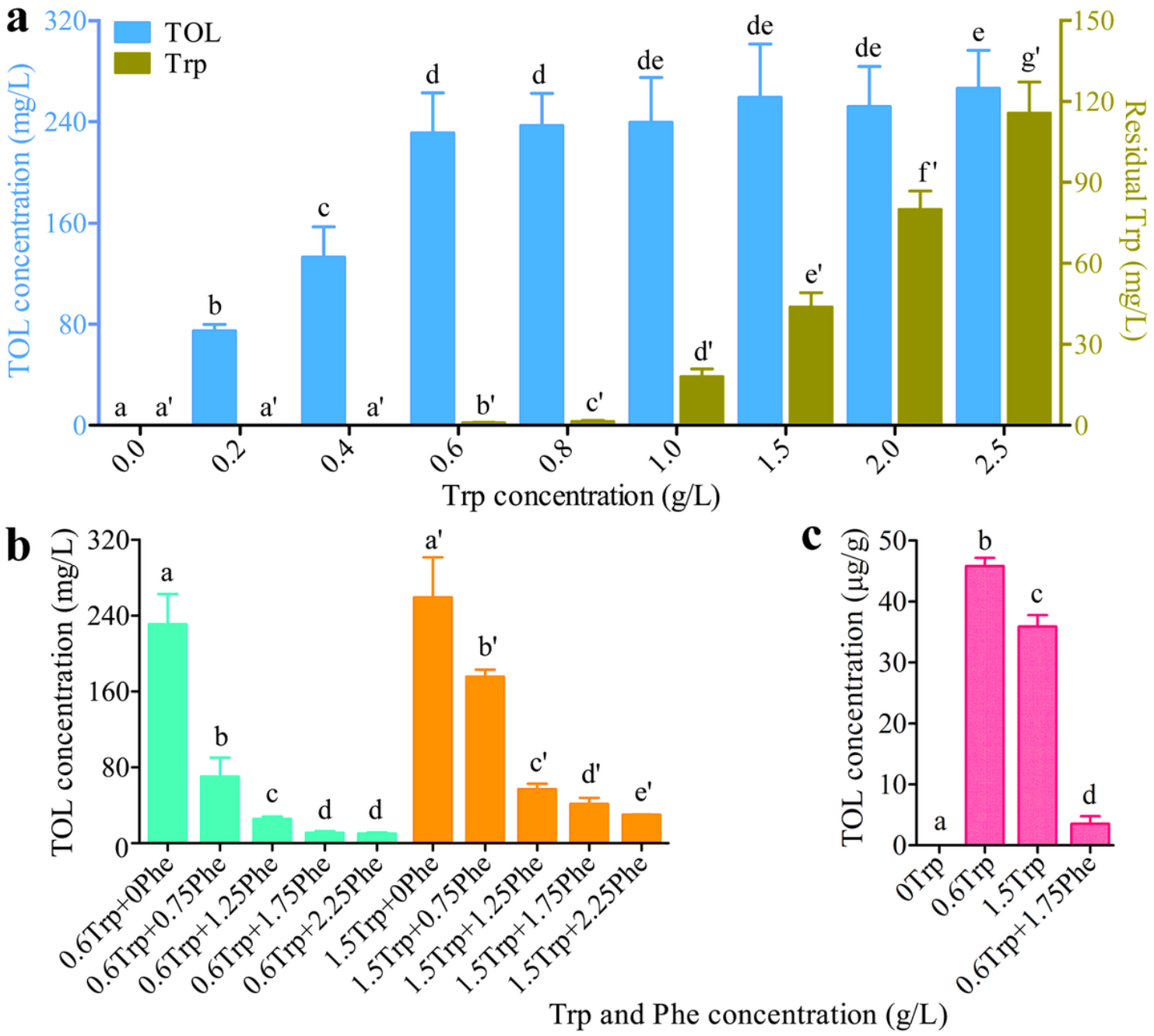

Figure 2

Effect of Trp and Phe on TOL production. a Extracellular TOL and residual Trp; b Extracellular TOL; c Intracellular TOL. Significant differences ($p < 0.05$) are indicated by different lowercase letters above the bars (a to e or a' to g').

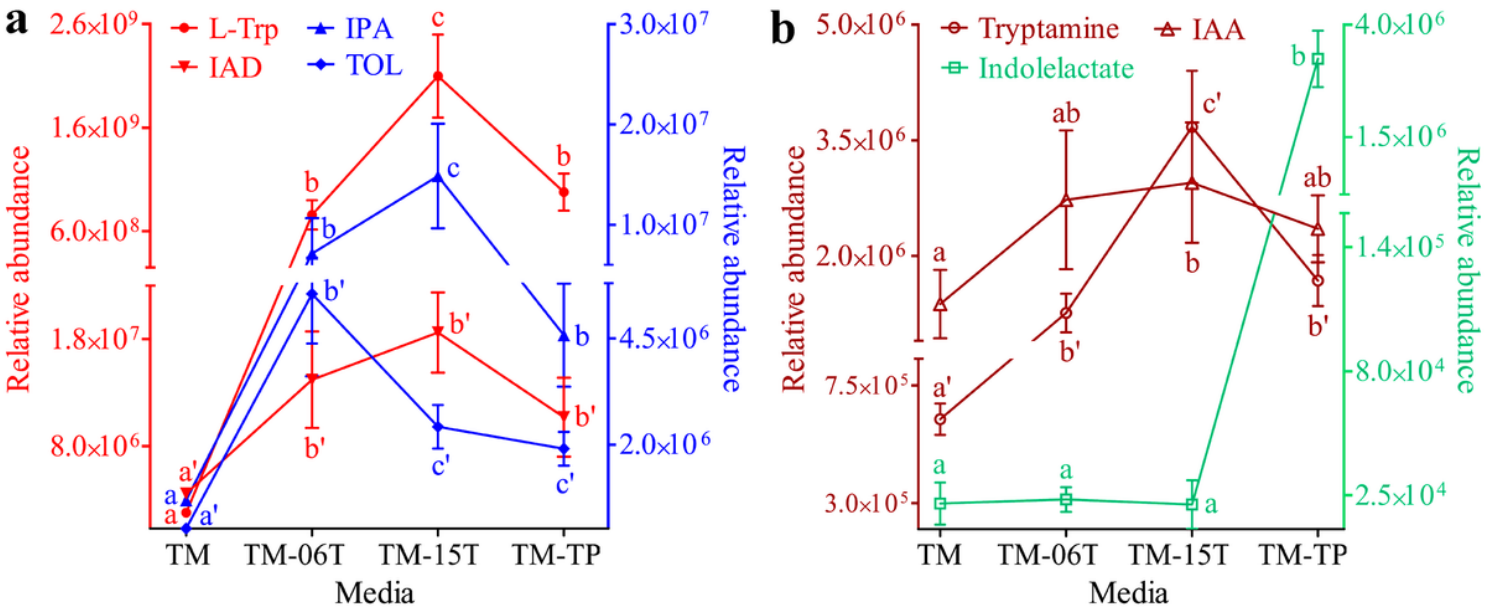

Figure 3

Abundance of DMs in the Ehrlich pathway (a) and the bypass pathway (b) of Trp metabolism. Mean values labelled with different lowercase letters are significantly different (fold change ≥2 and FDR <0.05).

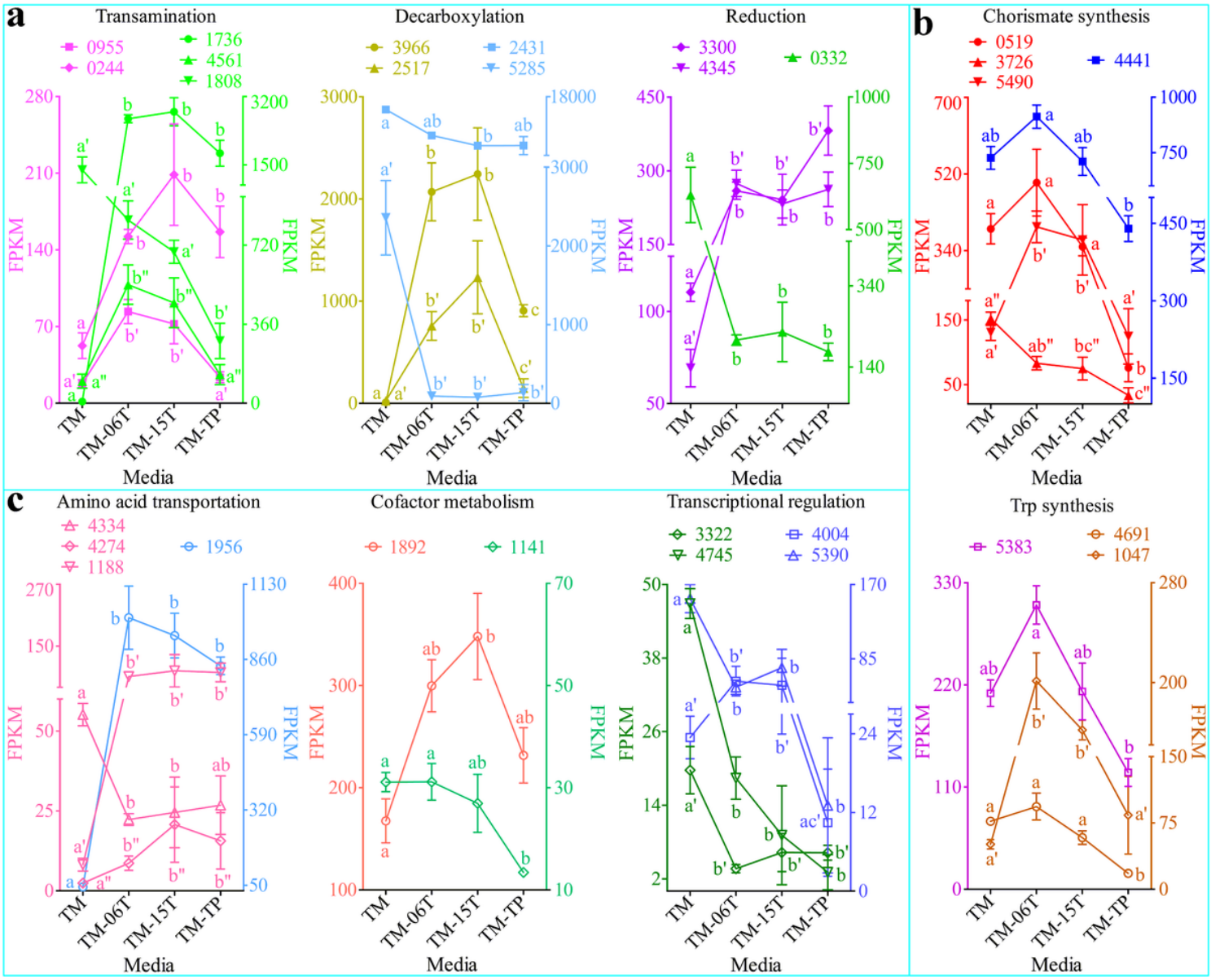

Figure 4

Expression levels of DEGs involved in TOL biosynthesis. a the Ehrlich pathway; b the de novo synthetic pathway; c the auxiliary pathway. Means marked with different lowercase letters (a to c, a' to c' or a" to c") differ significantly (fold change ≥2 and FDR <0.05). The description of genes represented by gene ID is shown in Table 1.

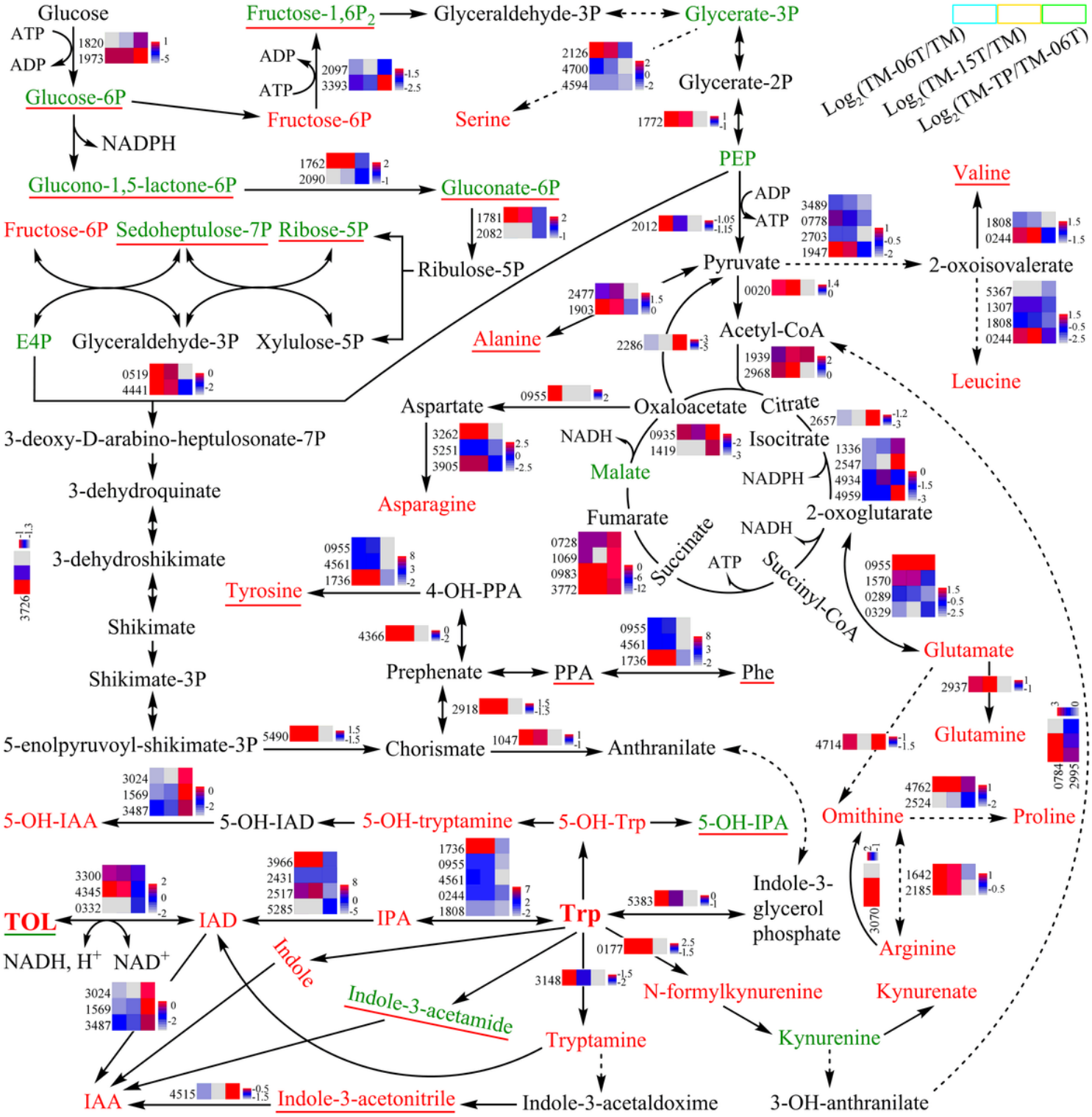

Figure 5

Schematic diagram of TOL biosynthetic pathways in S. cerevisiae. The up- and downregulated metabolites in TM-06T and/or TM-15T relative to TM are indicated in red and green fonts, respectively. If a metabolite is up- or downregulated in TM-06T vs. TM-TP, it is marked with a red or green underline, respectively. The expression pattern of each gene is represented by heat maps (as log2 fold change). Detailed information of DMs and DEGs in this picture can be found in Table S5.

Supplementary Files

This is a list of supplementary files associated with this preprint. Click to download.

- Fig.S1.tif
- Fig.S2.tif
- Fig.S3.tif
- Fig.S4.tif
- TableS1.doc
- TableS2.xls
- TableS3.docx
- TableS4.xlsx
- TableS5.xls
- TableS6.doc